

Stresses Inside Critical Nuclei

A. Cacciuto and D. Frenkel*

FOM Institute for Atomic and Molecular Physics, Kruislaan 407, 1098 SJ Amsterdam, The Netherlands

Received: September 24, 2004; In Final Form: November 11, 2004

The usual derivation of classical nucleation theory is inappropriate for crystal nucleation. In particular, it leads to a seriously flawed estimate of the pressure inside a critical nucleus. This has consequences for the prediction of possible metastable phases during the nucleation process. In this paper, we reanalyze the theory for crystal nucleation based on the thermodynamics of small crystals suspended in a liquid, due to Mullins (*J. Chem. Phys.* **1984**, *81*, 1436). As an illustration of the difference between the classical picture and the present approach, we consider a numerical study of crystal nucleation in binary mixtures of hard spherical colloids with a size ratio of 1:10. The stable crystal phase of this system can be either dense or expanded. We find that, in the vicinity of the solid–solid critical point where the crystallites are highly compressible, small crystal nuclei are less dense than large nuclei. This phenomenon cannot be accounted for by either classical nucleation theory or by the Gibbsian droplet model.

The experimental determination of crystal nucleation rates is one of the prime sources of information on the free energy of solid–liquid interfaces (see, e.g., ref 2). The link between the observable quantity (number of crystal nuclei formed per unit time per unit volume) and the surface free energy is usually given by classical nucleation theory (CNT). CNT contains two ingredients: the first is a thermodynamic estimate of the reversible work needed to make a critical nucleus (i.e., a nucleus that is equally likely to dissolve as it is to grow to macroscopic size). This reversible work defines the free energy of a critical nucleus. A system that contains a critical nucleus is at a local free-energy maximum. This is important for what follows, because it means that the free energy is invariant under infinitesimal exchanges of mass or volume between the nucleus and the parent phase. In particular, it means that chemical potentials of all species are constant throughout the system.³ The second ingredient of CNT is an estimate of the rate at which critical nuclei transform into macroscopic crystallites. In what follows, we focus on the equilibrium properties of critical crystal nuclei.

According to CNT, the free energy of a spherical nucleus that forms in a supersaturated solution contains two terms. The first term accounts for the fact that the solid phase is more stable than the liquid. This term is negative and proportional to the volume of the nucleus. The second term is a surface term. It describes the free energy needed to create a solid/liquid interface. This term is positive and proportional to the surface area of the nucleus. The (Gibbs) free energy of a spherical nucleus of radius R has the following form:

$$\Delta G = \frac{4}{3}\pi R^3 \rho_s \Delta\mu + 4\pi R^2 \gamma \quad (1)$$

where ρ_s is the number density of the bulk solid, $\Delta\mu$ the difference in chemical potential between the solid and the liquid, and γ is the solid/liquid surface free energy density. The function ΔG has a maximum at $R = 2\gamma/(\rho_s|\Delta\mu|)$ and the corresponding

height of the nucleation barrier is given by

$$\Delta G^* = \frac{16\pi}{3} \frac{\gamma^3}{(\rho_s|\Delta\mu|)^2} \quad (2)$$

One of the assumptions that is made in classical nucleation theory is that the crystal nucleus is incompressible. This assumption is not really necessary. It is not made in the so-called droplet model. In the Gibbsian droplet model of (liquid–vapor) nucleation, the free energy barrier for nucleation is computed by considering the effect of the Laplace pressure on the chemical potential of the critical nucleus. As the critical nucleus is in (unstable) equilibrium with the parent phase, it must have the same chemical potential. This is possible if the pressure inside the nucleus (P_n) is higher than the pressure P_p of the parent phase, such that $\mu_n(P_n) = \mu_p(P_p)$. This constraint on the chemical potential implies that

$$\mu_n(P_p + \Delta P) = \mu_p(P_p) \quad (3)$$

where μ_n denotes the chemical potential inside the nucleus and μ_p is the chemical potential of the surrounding metastable parent phase at a pressure $P_{\text{out}} \equiv P_p$.

In the droplet model, the pressure difference $\Delta P = P_n - P_p$ is assumed to be equal to the Laplace pressure $2\gamma/r_s$, where r_s is the radius of the surface of tension. Assuming that we know γ and the pressure dependence of the chemical potential of both phases, one can then compute r , the radius of the surface of tension of the critical nucleus, and the nucleation barrier itself ($4\pi\gamma r^2/3$). In contrast to CNT, the droplet model allows for the compressibility of the phase that nucleates. As the Laplace pressure is always positive, the droplet model predicts that small nuclei are necessarily denser than the corresponding bulk phase. However, as Gibbs already realized,⁴ the droplet model cannot be applied to crystallites as the excess pressure of crystals is not equal to $2\gamma/r_s$. The reason is that, for solid surfaces (or, more generally, surfaces of phases that have some degree of translational order) one should distinguish between the surface tension and the surface stress.

Mullins¹ has given a consistent thermodynamical description of small crystallites. Below, we briefly review the key results of Mullins' paper and then consider the implications for crystal nucleation.

Thermodynamics of Crystal Nuclei

The nucleation barrier is defined as the difference in grand potential between a system of (arbitrary) volume V containing a critical nucleus and a system with the same V , T , and μ containing only the metastable parent phase. For a liquid droplet, this barrier (that we denote by ΔG^*) is equal to

$$\Delta G^* = 4\pi r^2 \gamma - \frac{4\pi}{3} r^3 \Delta P \quad (4)$$

This expression is valid for any choice of r . If we choose for r the radius of the surface of tension, then we can use the Laplace equation for ΔP and we find

$$\Delta G^* = \frac{4\pi}{3} r^2 \gamma \quad (5)$$

As we shall see later, eq 5 also holds for crystal nucleation, but most of the other equations do not.

Let us next consider the case that the nucleus is not a liquid. We still assume a spherical nucleus. This is not essential, but it makes life easier. We consider a nucleus with radius r and volume $V_n = 4\pi r^3/3$, inside a system with total volume V_T , temperature T , and chemical potential μ (again, for convenience, I consider a one-component system). The choice of r is, at this stage, still arbitrary. The volume of the parent phase is $V_p = V_T - V_n$. The grand potential Ω of the system is given by

$$\Omega_T = \Omega_n + \Omega_p + \Omega_s \quad (6)$$

where Ω_n is the grand potential of the bulk phase inside the nucleus of volume $V - n$, Ω_p is the grand potential of the parent phase in volume V_p and Ω_s defines the grand potential of the surface. In equilibrium, the grand potential is a minimum and hence

$$\delta\Omega_n + \delta\Omega_p + \delta\Omega_s = 0 \quad (7)$$

If the parent is a liquid, we have

$$\delta\Omega_p = -P_p \delta V_p \quad (8)$$

where P_p is the ambient pressure in the liquid. The expression for $\delta\Omega_n$ is more subtle. We start from

$$d\Omega_n = dE_n - TdS_n - \mu dN_n \quad (9)$$

The energy of the nucleus can be written as $N_n e$, where N_n is the number of unit cells and e the energy per unit cell. Hence

$$dE_n = e dN_n + N_n de \quad (10)$$

This equation expresses the fact that, for crystals, the number of unit cells is an independent thermodynamic variable. Similar expressions can be written for the other extensive properties of the nucleus (S , V , N , and Ω). The variation de can be written as

$$de = T ds - P_n dv + \mu dv \quad (11)$$

where v is the volume of particles per unit cell (this number is not fixed, to allow for vacancies and interstitials).

We can then write eq 10 as

$$\begin{aligned} dE_n &= N_n(T ds - P_n dv + \mu dv) + e dN_n \\ &= (TdS - Ts dN_n) - (P_n dV - P_n v dN_n) + \\ &\quad (\mu dN - \mu v dN_n) + e dN_n \\ &= T dS - P_n dV + \mu dN + (\omega + P_n v) dN_n \end{aligned} \quad (12)$$

where we have defined the grand potential per unit cell as

$$\omega = e - Ts - \mu v \quad (13)$$

With this expression for dE_n , we can write eq 9 as

$$d\Omega_n = -P_n dV_n + (\omega + P_n v) dN_n \quad (14)$$

The basic variational eq 7 then becomes

$$-P_n dV_n - P_p dV_p + (\omega + P_n v) dN_n + d\Omega_s = 0 \quad (15)$$

We now consider separately two cases. First we consider the situation that v is constant and then the case where N_n is constant.

Variation at Constant v . If v is constant, $dV_n = v dN_n$ and the variational equation becomes

$$(P_p + \omega/v) dV_n + dA \omega_s = 0 \quad (16)$$

where we have defined $\omega_s = \Omega_s/A$, with A being the surface area of the nucleus. Similarly, we define $\omega_p = \Omega_p/V_p$ and $\omega_n = \Omega_n/V_n = \omega/v$. As the parent phase is a liquid, $\omega_p = -P_p$ depends only on T and μ , but as the nucleating phase is a solid, ω_n depends on T , μ , and v . At fixed T , μ , and v , the variation in Ω_T is therefore

$$\delta\Omega_T = \omega_n \delta V_n - \omega_p \delta V_n + \frac{\partial A \omega_s}{\partial V_n} \delta V_n = 0 \quad (17)$$

As this must hold for arbitrary δV_n , we obtain

$$\begin{aligned} \omega_p - \omega_n &= \frac{1}{r^2} \frac{\partial r^2 \omega_s}{\partial r} \\ &= \frac{2}{r} \left(\omega_s + \frac{r}{2} \frac{\partial \omega_s}{\partial r} \right) \end{aligned} \quad (18)$$

This equation can be integrated to yield (after rearrangement)

$$A \omega_s + V_n (\omega_n - \omega_p) = W \quad (19)$$

where the integration constant W is (of course) independent of r . As $\Omega_T = \omega_n V_n + \omega_p V_p + A \omega_s$, it follows that

$$W = \Omega_T - \omega_p V_T \quad (20)$$

i.e., it is the difference of grand potential between a system of volume V_T containing a critical nucleus and a system of the same volume containing the parent phase. In other words W corresponds to the reversible work needed to make a critical nucleus.

Thus far, we have not specified r . The physical properties of the crystal (nucleus) do not depend on the particular choice of the dividing surface. As in the case of a liquid nucleus (eq 5),

we now choose r to be the radius of the surface of tension, such that

$$\frac{\partial \omega_s}{\partial r} = 0 \quad (21)$$

This is possible for $\omega_n < \omega_p$ (i.e., if n is the stable phase) as can be seen by differentiating eq 19. The solution of eq 21 is

$$r^* = \left(\frac{3W}{2\pi(\omega_p - \omega_n)} \right)^{1/3} \quad (22)$$

We now define γ as $\omega_s(r^*)$. For $r = r^*$, we then have

$$\omega_p - \omega_n = \frac{2\gamma}{r^*} \quad (23)$$

and

$$W = \gamma A^*/3 \quad (24)$$

Note that eqs 23 and 24 are essentially the same as for liquid nuclei. It is interesting that, whereas almost all thermodynamic properties of crystal nuclei differ from the expression given by CNT, the expression for the barrier height is exactly the one given by Gibbs (ref 4, p 258, eq 560—although, as we shall see, the second part of this equation does not hold for crystal nuclei).

Variation at Constant N_n . All results obtained thus far still depend on v , the volume per unit cell that was held constant. Now we consider variations in v at constant N_n . Then

$$d\omega_s = \frac{\partial \omega_s}{\partial r} dr + \frac{\partial \omega_s}{\partial v} dv \quad (25)$$

For any value of v , we can choose r such that $\partial \omega_s / \partial r = 0$. Denoting (as before) $\omega_s(r^*)$ as γ , we then get

$$d\omega_s = \frac{d\gamma}{dv} dv \quad (26)$$

Then, using eq 15 at constant N_n , we get

$$P_n - P_p = \gamma \frac{da}{dv} + a \frac{d\gamma}{dv} \quad (27)$$

Using $da/dv = 2/r$ and $a/v = 3/r$, we can write

$$P_n - P_p = \gamma \frac{da}{dv} + a \frac{d\gamma}{dv} = \left(\gamma + \frac{3}{2} v \frac{d\gamma}{dv} \right) \frac{2}{r} \equiv \frac{2f}{r} \quad (28)$$

where the last equality defines the surface stress f . Note that the expression for the barrier height (eq 24) involves the surface free-energy density γ , but the expression for “Laplace” pressure of the crystal nucleus involves the surface stress f . This is a crucial departure from CNT and the droplet model. Combining eq 28 with eq 23 and using the fact that $\omega_p = -P_p$ we get

$$P_n + \omega_n = \frac{3v}{r} \frac{\partial \gamma}{\partial v} \quad (29)$$

This equation will be used in the next section. There we will use it in the form

$$v \frac{\partial \omega_n}{\partial v} = - \frac{3v}{r} \frac{\partial \gamma}{\partial v} \quad (30)$$

or

$$\frac{\partial \omega_n}{\partial v} = - \frac{3}{r} \frac{\partial \gamma}{\partial v} \quad (31)$$

Consequences for Nucleation

To study the effect of surface stress on nucleation, we start from eq 31 above and eq 23 written as

$$P_p + \omega_n = - \frac{2\gamma}{r^*} \quad (32)$$

For a bulk solid at coexistence, ω_n is equal to $-P_p$. However, in a small nucleus, ω_n changes due to elastic deformation. We can write:

$$\omega_n = -P_n^0 + \frac{1}{2} B \epsilon^2 + O(\epsilon^3) \quad (33)$$

where $\epsilon \equiv (v - v_0)/v_0$ is a measure for the elastic strain (for convenience, we have assumed that the crystal nucleus is elastically isotropic) and P_n^0 is the pressure where the chemical potential of the bulk solid would be equal to that of the parent phase. The linear term in ϵ is absent because ω is at a minimum for a bulk solid in equilibrium. We can also expand γ in powers of ϵ :

$$\gamma = \gamma_0 + \gamma_1 \epsilon + \frac{\gamma_2}{2} \epsilon^2 + O(\epsilon^3) \quad (34)$$

Using eqs 32 and 31, we can write

$$({}^{2/3}) \gamma \frac{\partial \omega_n}{\partial v} = (P_p + \omega_n) \frac{\partial \gamma}{\partial v} \quad (35)$$

We can write this explicitly in terms of the strain ϵ . To second order, we get

$$({}^{2/3}) (\gamma_0 + \gamma_1 \epsilon) \frac{\partial ({}^{1/2}) B \epsilon^2}{v_0 \partial \epsilon} = (P_p - P_n^0 + ({}^{1/2}) B \epsilon^2) \frac{(\partial \gamma_1 \epsilon + ({}^{1/2}) \gamma_2 \epsilon^2)}{v_0 \partial \epsilon} \quad (36)$$

or

$$({}^{2/3}) (\gamma_0 + \gamma_1 \epsilon) B \epsilon = (P_p - P_n^0 + ({}^{1/2}) B \epsilon^2) (\gamma_1 + \gamma_2 \epsilon) \quad (37)$$

Equating the terms to lowest order in ϵ , we find:

$$({}^{2/3}) \gamma_0 B \epsilon = (P_p - P_n^0) \gamma_1 \quad (38)$$

or

$$\epsilon = - \frac{3(P_n^0 - P_p) \gamma_1}{2 \gamma_0 B} \quad (39)$$

Using eq 32, we then find (to linear order in ϵ)

$$r^* = 2 \frac{(\gamma_0 + \gamma_1 \epsilon)}{P_n^0 - P_p} \quad (40)$$

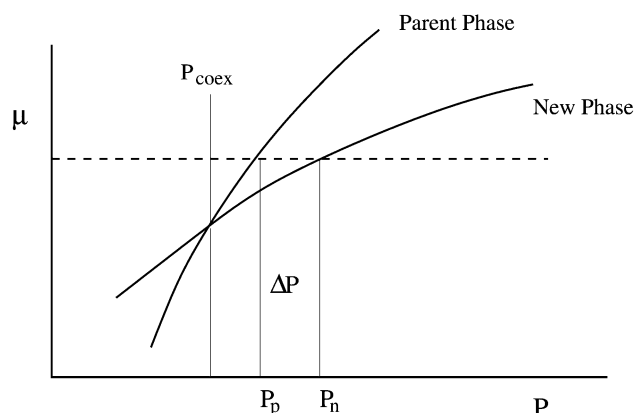


Figure 1. Critical nucleus in an (unstable) equilibrium with the parent phase. This implies that the chemical potential is constant throughout the system. The figure shows a schematic drawing of the chemical potential of the stable and metastable phases of a system close to a first-order phase transition, as a function of pressure. At coexistence, the curves cross. If one phase is supersaturated ($P_m > P_{\text{coex}}$), then the pressure P_s of the stable phase inside the critical nucleus must be such that its chemical potential is equal to that of the metastable phase.

and the expression for the nucleation barrier (24) becomes (to the same order):

$$W = \frac{4\pi}{3}(\gamma_0 + \gamma_1\epsilon) \left(2 \frac{(\gamma_0 + \gamma_1\epsilon)^2}{P_n^0 - P_p} \right) \quad (41)$$

Note that all these equations are different from the expression for vapor–liquid nucleation except Gibbs’s expression for the barrier height. Why is the pressure inside a nucleus important? One reason is that the pathway for crystal nucleation can be strongly influenced by the presence of metastable phases. This observation dates back to Ostwald, who formulated his famous “step” rule stating that the crystal phase that nucleates from the supersaturated parent phase need not be the one that is thermodynamically most stable, but the one that is closest in free energy to the parent phase.⁵ Why would a solid phase that is metastable in the bulk become the most stable in a small nucleus? There are two simple—not necessarily exclusive—mechanisms by which this could happen. The first scenario is that the surface free energy of the metastable solid phase is less than that of the stable phase. Then, according to eq 1, small crystallites of the metastable will always be more stable than those of the stable phase. A second scenario is that the relative stability of the stable and metastable solid phases is reversed inside the nucleus, due to the Laplace pressure (see Figure 2). As we have shown above, the pressure inside the nucleus can be both higher and lower than the ambient pressure (depending on the sign of the surface stress).

As an illustration of the effect of surface stress on the structure of the critical nucleus, we consider crystal nucleation in the vicinity of a (isostructural) solid–solid critical point.⁶ Isostructural solid–solid transitions are expected to occur in crystalline alloys near a substitutional order–disorder transition or in systems of hard colloidal particles with a short-ranged attraction.^{7–10} Here, we consider the latter case. Depending on the range of attraction, the solid–solid critical point may either be located in a stable or in a metastable part of the phase diagram. Simulations by Dijkstra indicate that this is the case for mixtures of large and small hard colloids.¹⁰ The small colloids (diameter σ_s) induce an effective attraction between the large colloids (diameter σ_l). The range of the attraction is determined by the size of the small colloids. For a size ratio q

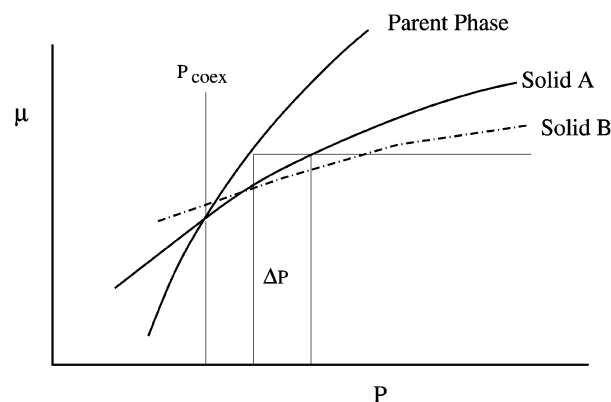


Figure 2. Schematic drawing of the relative stability of two crystal phases, as a function of the pressure inside the nucleus. At coexistence, solid A is stable and B is metastable. However, at the pressure where the chemical potential inside the nucleus is equal to that of the supersaturated parent phase, solid B is more stable than solid A.

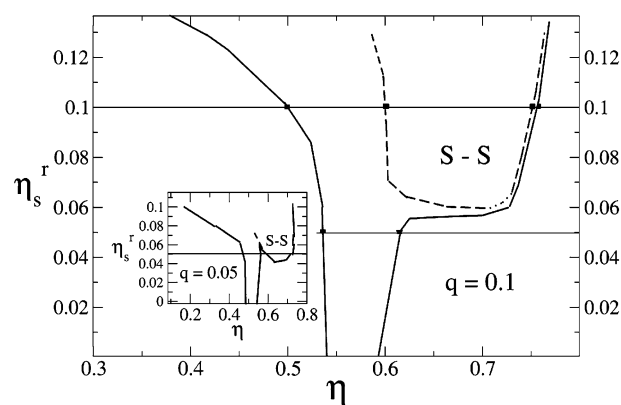


Figure 3. Sketch of the phase diagram of a binary hard sphere mixture of volume fraction η for $q = 0.1$ and $q = 0.05$ (inset) obtained from data reported in ref 10. η_s^r is the volume fraction of a reservoir of small spheres in contact with the system. The dashed curves indicate the metastable solid–solid phase. Horizontal lines mark the values of η_s^r where we performed simulations.

$\equiv (\sigma_s/\sigma_l) = 0.05$, the phase diagram exhibits a stable isostructural critical point. For $q = 0.1$ the range of attraction is longer and the isostructural critical point moves to the metastable region beyond the melting curve (see Figure 3). We performed Monte Carlo simulations to investigate how the presence of a metastable critical point in the crystal phase affects the early stages of the nucleation process. The direct numerical simulation of a highly asymmetric hard-sphere mixture is computationally demanding.¹¹ However, for q sufficiently small, we can account for the effect of the small spheres by using an effective potential.^{10,12} The range and strength of this interaction depend on the size and concentration of the small spheres. The effective pair interaction between a pair of large colloids in contact with a reservoir of small spheres at volume fraction η_s^r is approximately given by^{10,12}

$$\beta\phi_{\text{eff}}(R) = \begin{cases} -\frac{1+q}{2q}[3\lambda 2\eta_s^r + (9\lambda + 12\lambda 2)(\eta_s^r)^2 + (36\lambda + 30\lambda 2)(\eta_s^r)^3] & (\sigma_l < R < \sigma_l + \sigma_s) \\ 0 & (R > \sigma_l + \sigma_s) \end{cases} \quad (42)$$

where R is the distance between the large colloids, $\lambda \equiv R/\sigma_s$ —

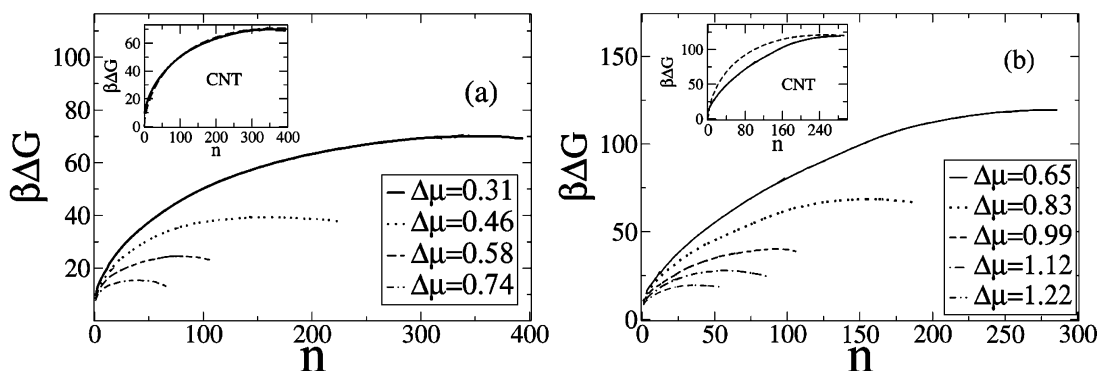


Figure 4. Free energy crystal nucleation barriers $\Delta G(n)$ as a function of the nucleus size for $q = 0.1$ at (a) $\eta_s^r = 0.05$ and (b) $\eta_s^r = 0.1$ for different values of the chemical potential. Error-bars on ΔG are of the order of $1 k_B T$. The inset shows a comparison between the highest computed barrier and form predicted by CNT.

$1/q - 1$ and $\beta \equiv 1/k_B T$. We focus on small values of η_s^r , where it is permissible to ignore higher order corrections to this expansion.¹²

We performed constant-pressure Monte Carlo simulations of binary hard-sphere mixture with a size ratio $q = 0.1$ at two different values of η_s^r . For $\eta_s^r = 0.05$, there is only one crystal phase. For $\eta_s^r = 0.1$, a metastable crystal phase exists between the fluid phase and the equilibrium crystal phase (see Figure 3). We started from a stable liquid suspension of $N = 3375$ large colloids and compressed it beyond the freezing density. We then computed ΔG , the free-energy barrier for crystal nucleation, as a function of the size n of the crystal nucleus (see ref 13 for technical details). This calculation was repeated at different super-saturations $\Delta\mu = |\mu_{\text{sol}} - \mu_{\text{liq}}|$ (where μ_{sol} (μ_{liq}) are the chemical potentials of the solid and liquid phases respectively). Figure 4 shows the computed crystal-nucleation barriers as a function of nucleus size n for different values of $\Delta\mu$.

It is instructive to compare the shape of the computed nucleation barriers with the functional form predicted by classical nucleation theory (CNT)²:

$$\Delta G = \gamma_{\text{ls}} S - |\Delta\mu| \rho_s V \quad (43)$$

where S is the surface area of the crystal nucleus, V is its volume, and ρ_s is the density of the crystal at coexistence. Figure 4 shows that there is a striking difference in behavior between the systems with and without a metastable solid phase: in the absence of a metastable solid phase (Figure 4a), classical nucleation theory accounts well for the shape of the nucleation barrier. However, in the presence of a metastable solid phase (Figure 4b), CNT cannot reproduce the shape of the nucleation barrier.

One of the central assumptions of CNT is that the structure of the crystal nucleus is that of the stable bulk phase at coexistence. In the presence of a metastable solid phase, this assumption is violated. This is most easily seen by considering the density of crystal nuclei as a function of their size. As there is some ambiguity in the definition of ρ_c , the number density of a small crystallite, we computed this quantity in three different ways. A rough estimate can be obtained by locating the center of mass of the cluster and then counting the number of particles inside spheres of increasing radius. A second estimate is obtained by matching the distribution of the nearest-neighbors distances inside a nucleus to that of a bulk crystal. The density of the bulk crystal that gives the best match defines ρ_s . A third approach was to perform a Voronoi construction around each particle inside the cluster. The density was then defined as the

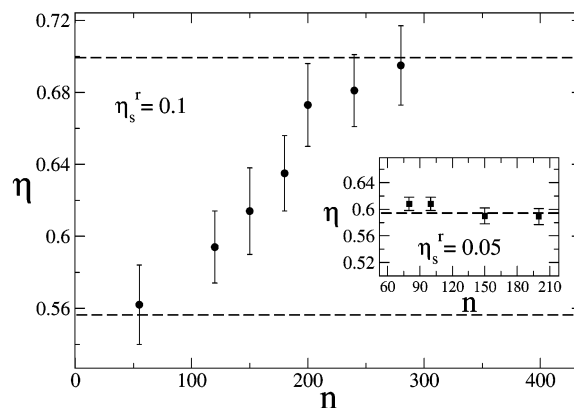


Figure 5. Crystal clusters volume fraction as a function of their size for a binary mixture with $q = 0.1$ and $\eta_s^r = 0.1$ at $\Delta\mu = 0.65$. The dashed lines indicate the location of the metastable solid-solid phase. The critical nucleus contains approximately $n \sim 290$ particles. The inset graphs the quantities for $\eta_s^r = 0.05$ at $\Delta\mu = 0.31$. Error bars are large enough to include the estimate obtained with the three methods described in the text.

number of particles inside the nucleus divided by the sum of the volumes of the Voronoi polyhedra. Figure 5 shows the density of crystal nuclei of increasing size at $\eta_s^r = 0.1$ and $\Delta\mu = 0.65$. The densities were computed using the three methods described above and the difference between the results for different methods falls within the error bars. For each size, we considered a sample of 100 different clusters.

The figure shows that the density of clusters increases with size. To rule out that the observed density change is a trivial finite-size effect, we repeated the same calculation for crystal nuclei at $\eta_s^r = 0.05$ where no metastable solid phase is present. The inset of Figure 5 shows that, in that case, the density of the crystal nuclei is effectively independent of size. Moreover, for mixtures with a size ratio $q = 0.05$ (short-ranged effective interaction) the low-density solid-phase becomes stable¹⁰ near $\eta_s^r = 0.05$, while the high-density solid phase is metastable (see Figure 3). In that case, we always found that the crystal nuclei had densities corresponding to the low-density phase. Figure 5 only gives information about the average density of the nucleus. We tested whether the density of the solid was constant throughout the nucleus. To this end, we generated 100 well-equilibrated configurations of a 280-particle crystal nucleus. The overall density of the crystallite follows from Figure 5. To probe the local density, we computed the distribution of interparticle distances $P(d)$ in this cluster for different spherical shells around the center of mass of the cluster. If the density or structure varies as a function of radius, we should expect to see

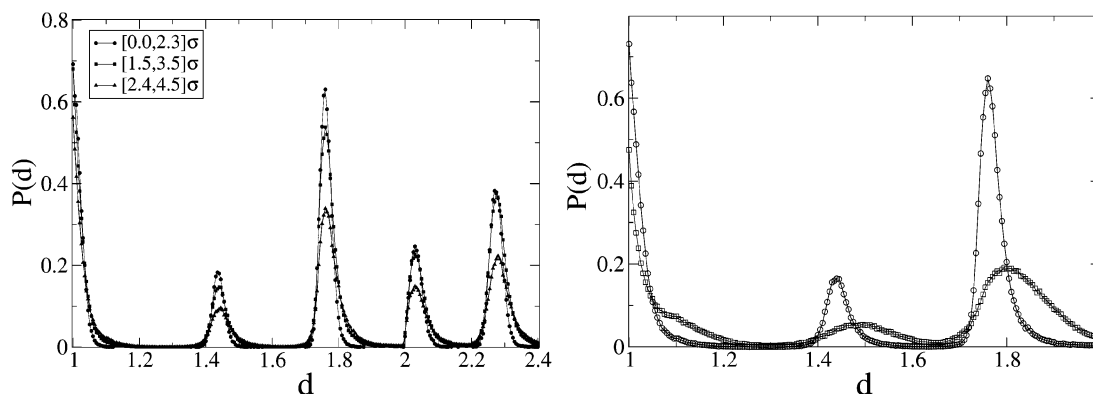


Figure 6. Left-hand side: interparticle distance distributions $P(d)$ for three different spherical shells inside a 280-particle crystalline nucleus. Stars: $0 < r < 2.3\sigma$. Squares: $1.5\sigma < r < 2.5\sigma$. Triangles: $2.4\sigma < r < 4.5\sigma$. Right-hand side: $P(d)$ for an expanded ($\rho = 0.56$, squares) and a condensed ($\rho = 0.70$, circles) bulk crystal. This figure shows that the positions of the peaks of $P(d)$ depend clearly on density.

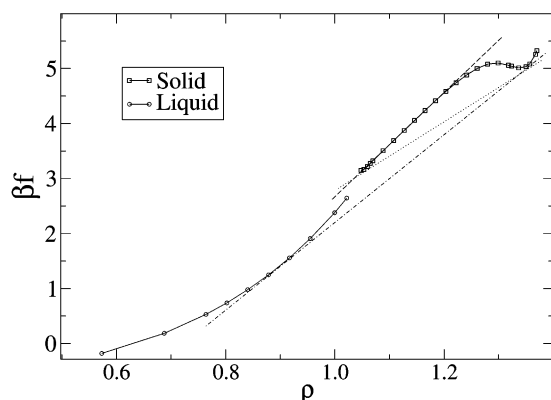


Figure 7. Density dependence of the free-energy density of a binary colloidal mixture with $q = 0.1$ and $\eta_s^f = 0.1$. Using the common tangent construction, we can derive the densities of the coexisting phases, and the pressures at which this coexistence occurs. From the figure we deduce that there is solid–liquid equilibrium for $\rho_{\text{liq}} \approx 0.46$, $\rho_{\text{sol}} \approx 0.706$, and reduced pressure $P \approx 5.9$ (common tangent: dash-dot). Metastable solid–solid coexistence occurs for $\rho_{\text{exp}} \approx 0.556$, $\rho_{\text{dense}} \approx 0.705$, and $P \approx 3.6$ (common tangent: dotted line). The maximum pressure that the expanded metastable solid can withstand can be estimated from the drawn line in the figure: $P \approx 6.76$.

the positions of the peaks in $P(d)$ vary from one shell to the next. In fact, as can be seen from the left-hand side of Figure 6, the positions of the peaks in $P(d)$ are the same throughout the nucleus. For the sake of comparison, the right-hand side of Figure 6 shows that the $P(d)$'s for the high- and low-density crystals are clearly different.

At the pressures for which we performed the simulations, the dense solid is, in the bulk, always more stable than the metastable expanded solid. If the pressure of the nucleus were determined by the usual Laplace expression, it would be hard to understand how small crystal nuclei can have a lower density than large nuclei. To illustrate this, Figure 7 shows the free energy density f of the solid and liquid phases of the binary mixture at $q = 0.1$ and $\eta_s^f = 0.1$. In the figure, we show the common tangent constructions to obtain equilibrium densities and pressures of stable (Liquid–Solid) and metastable (solid–solid) states. In addition, the figure shows that the bulk expanded solid is mechanically unstable for reduced pressures larger than $P \approx 6.76$. Yet, in our simulations of crystal nucleation, the reduced pressure was never less than $P = 9$. If crystal nucleation were similar to droplet nucleation, then we would have to add the Laplace pressure to the ambient pressure to get the pressure inside the nucleus. Clearly, this would make the expanded phase even less stable and hence we must conclude that the usual

Laplace-pressure argument does not hold for crystal nucleation. However, the observed behavior is precisely what we should expect in a crystallite with negative surface stress.

Analysis of Simulation Results

In our simulations, we can measure the density of the nucleus and this allows us to compute the elastic strain ϵ . We know the pressure P_p of the parent phase. In addition, using the Gibbs–Duhem equation, we can compute P_n^0 , the pressure where the chemical potential of the bulk solid would be equal to that of the parent phase. From the equation of state of the solid, we can compute the bulk modulus B at the pressure P_n^0 . In addition, the simulations yield the barrier height W . From these numbers, we first obtain the ratio γ_1/γ_0

$$\frac{\gamma_1}{\gamma_0} = - \frac{2\epsilon B}{3(P_n^0 - P_p)} \quad (44)$$

and this then allows us to compute

$$\frac{r^*}{\gamma} = \frac{2}{P_n^0 - P_p} \quad (45)$$

We then write

$$W = \frac{16\pi}{3} \gamma^3 (P_n^0 - P_p)^{-2} \quad (46)$$

or

$$\gamma^3 = \frac{3W}{16\pi} (P_n^0 - P_p)^2 \quad (47)$$

This equation then allows us to compute γ , and then, using eq 44, we obtain γ_0 and γ_1 . Finally, using eq 48

$$P_n - P_p = \left(\gamma_0 + \epsilon \gamma_1 + \frac{3}{2}(1 + \epsilon) \right) (\gamma_1 + \gamma_2 \epsilon) \frac{2}{r^*} \quad (48)$$

we can compute the actual pressure inside the nucleus. To lowest order, the presence of surface stress lowers the pressure in the critical nucleus by an amount

$$\frac{P_n - P_n^0}{P_n^0 - P_p} = \frac{3\gamma_1}{2\gamma_0} = - \frac{B\epsilon}{P_n^0 - P_p} \quad (49)$$

As we can determine γ from the (experimentally accessible) barrier height, we can then obtain r^* and hence the volume V_c of the critical nucleus. Using the nucleation theorem, we can obtain $\Delta N \equiv V_c(\rho_c - \rho_L)$ from experiments. As ρ_L is known, we can then derive ρ_c . This makes possible to determine the density of the nucleus from experiments.

Solid–Solid Transition

Next, consider the situation where the solid under consideration can undergo an isostructural solid–solid transition.

Let us assume that the expanded solid corresponds to a deformation ϵ_e . In that case, we can approximate Using the

$$\begin{aligned}\omega_n &= -P_n^0 + \frac{1}{2}B\epsilon^2 \quad (\epsilon < \epsilon_e/2) \\ &= -P_n^0 + a + \frac{1}{2}B(\epsilon - \epsilon_e)^2 \quad (\epsilon > \epsilon_e/2)\end{aligned}$$

definition $\Delta\epsilon = \epsilon - \epsilon_e$, eq 37 becomes

$$(\frac{2}{3})(\gamma_0 + \gamma_1\epsilon_e)B\Delta\epsilon \approx (P_p - P_n^0 + a)\gamma_1 \quad (50)$$

In the present case (hard spheres with short-ranged attraction), the derivative $(\partial\gamma/\partial\rho)$ is presumably large and positive. There are two ways to reach this conclusion. One is based on a thermodynamic perturbation theory estimate of the contribution of an attractive interaction on the (hard-sphere) solid–liquid interfacial free-energy density. As this correction has the form $\Delta\gamma = c \times (\Delta\rho)^2$, where $\Delta\rho$ is the density difference between solid and liquid and c is a positive constant, it is clear that $(\partial\gamma/\partial\rho) > 0$. As perturbation theory works best for weak, long-ranged attractive forces, the present estimate is less appropriate for the binary colloid system. In that case, we can estimate the surface free-energy density from the latent heat of fusion (using Turnbull's rule—see, e.g., ref 2). The latent heat of fusion of particles with short ranged interaction can be estimated using the van der Waals theory for solids, due to Daanoun et al.⁸ This route too leads to the conclusion that $(\partial\gamma/\partial\rho) > 0$. For sufficiently strong, short ranged attractions, the surface stress becomes negative and so does ΔP . The theoretical analysis of Mullins¹ shows that, to lowest order in the crystal strain, the density change of a crystalline nucleus is given by

$$\frac{\rho - \rho_0}{\rho_0} = -\left(\frac{\partial\gamma}{\partial\rho}\right)_0 \frac{3\rho_0}{rB} \quad (51)$$

where B is the bulk modulus of the solid. In our simulations, we compute the equation of state of the solid and, from this, we can derive B . To linear order in the strain, the radius of the critical nucleus is related to the supersaturation through:

$$r = \frac{2\gamma}{P_0^S(\mu) - P^L(\mu)} \quad (52)$$

where $P_0^S(\mu)$ and $P^L(\mu)$ are the pressures of the bulk solid and of the metastable liquid at chemical potential μ . γ is the surface free-energy density of the strained nucleus. Note that $\Delta\rho$ is negative: hence the solid indeed expands. This expansion is inversely proportional both to the radius of the nucleus and to the bulk modulus of the crystal. As B vanishes at the solid–solid critical point, the value of B in eq 52 can be small for nuclei that form close to this critical point. The expansion of

the nucleus can therefore be large, in particular for small r . This is precisely what we observe in the simulations. The observed expansion of small nuclei is in stark contrast with the predictions of both CNT and the droplet model.

We can make a rough estimate of the effect of surface stress on the excess pressure inside the nucleus. To lowest order in the strain, the strain-induced pressure change ΔP is given by

$$\Delta P = \frac{B(\rho - \rho_0)}{\rho_0} \quad (53)$$

This is a large correction. For the small, expanded nuclei that we observe, $\Delta P/P_L \sim -20$. However, this estimate is not realistic. In the vicinity of a solid–solid transition, higher powers of the strain should be included to obtain a more accurate estimate of the strain-induced pressure change. We have not attempted this here: our objective was simply to show that surface stress has a large effect on the internal pressure of crystal nuclei. The effect of surface stress on the density of crystal nuclei should be experimentally observable in the nucleation of compressible crystals, such as colloids with short-ranged attraction and globular proteins. Such an expansion can be determined by application of the nucleation theorem^{14,15} to the temperature or (osmotic) pressure dependence of the nucleation rate. In the case of protein crystallization, a better understanding of the role of surface stress made be of practical importance. Short-ranged attractions could, for instance, favor the nucleation of a crystal form that is less dense than the one that is thermodynamically stable. One can even speculate about the effect of surface stress on single proteins. If we view the native state of a protein as a single-chain crystal, then it is obvious that the packing density of the crystal will be affected by surface stress. To our knowledge, no systematic studies of this effect exist. Even for vapor–liquid nucleation there may be residual surface-stress effects in small droplets because such small system may exhibit layering. This may explain the puzzling inconsistencies between the thermodynamical surface of tension and the mechanical surface of tension, as observed in simulations.¹⁶ It would be very interesting to have a systematic theoretical analysis of the effect of surface stress in small droplets—for instance in the context of density-functional theory.

Acknowledgment. A.C. thanks I. Coluzza for helpful suggestions. The work of the FOM Institute is part of the research program of FOM and is made possible by financial support from The Netherlands organization for Scientific Research (NWO) and by contracts NWO-04-016-022 and EU-MRTN-CT-2003-504712. Finally, D.F. thanks David Chandler for his enthusiasm and support.

References and Notes

- (1) Mullins, W. W. *J. Chem. Phys.* **1984**, *81*, 1436–1442.
- (2) Kelton, K. F. *Solid State Physics* **1991**, *45*, 75.
- (3) We limit our discussion to a one-component system. Moreover, we assume that, during an exchange of particles between the nucleus and the bulk, the number of particles in the surface is not changed. Often, it is assumed that the total adsorption is zero, in which case the equimolar surface and the surface of tension are the same.
- (4) *The Scientific Papers of J. Willard Gibbs. Volume, I. Thermodynamics*; Ox Bow Press: Woodbridge, CT, 1993.
- (5) Ostwald, W. Z. *Phys. Chem.* **1897**, *22*, 289–330.
- (6) Cacciuto, A.; Auer, S.; Frenkel, D. *Phys. Rev. Lett.* **2004**, *93*, 166105.
- (7) Bolhuis, P.; Frenkel, D. *Phys. Rev. Lett.* **1994**, *72*, 2211–2214.
- (8) Daanoun, A.; Tejero, C. F.; Baus, M. *Phys. Rev. E* **1994**, *50*, 2913–2924.
- (9) Likos, C. N.; Nemeth, Z. T.; Löwen, H. *J. Phys.: Condens. Matter* **1994**, *6*, 10965–10975.

- (10) Dijkstra, M.; van Roij, R.; Evans, R. *Phys. Rev. E* **1999**, *59*, 5744–5771, *Phys. Rev. Lett.* **1998**, *81*, 2268–2271.
- (11) Biben, T.; Bladon, P.; Frenkel, D. *J. Phys.: Condens. Matter* **1996**, *8*, 10799–10821.
- (12) Götzelmann, B.; Evans, R.; Dietrich, S. *Phys. Rev. E* **1998**, *57*, 6785–6800.
- (13) Auer, S.; Frenkel, D. *J. Chem. Phys.* **2004**, *120*, 3015–3029.
- (14) Viisanen, Y.; Strey, R.; Reiss, H. *J. Chem. Phys.* **1993**, *99*, 4680–4692.
- (15) Oxtoby, D. W.; Kashchiev, D. *J. Chem. Phys.* **1994**, *100*, 7665–7671.
- (16) ten Wolde, P. R.; Frenkel, D. *J. Chem. Phys.* **1998**, *109*, 9901–9918.